



ISSN: 0067-2904

Effect of Shaliness on Water Saturation: A Case Study of TN Field Niger Delta

Abbey CHukwuemeka Patrick*¹, Orenuga, Israel Abayomi², Okpogo, Emele Uduma²

¹Department of Petroleum Chemistry and Physics, School of Arts and Science, American University of Nigeria Yola.

²Geosciences Department, University of Lagos

Abstract

This study was carried out to estimate the effect of shaliness on water saturation from TN field of Niger Delta. The conventional Archie and the Shaly-sand water saturation models were used in the evaluation of wells. Two sand layers (Sand 01 and 02) were mapped with thicknesses range from 76.8ft to 119.3ft across the three wells for Sand 01 and 187.5 to 339.9ft across wells TN_1 and TN_4 for Sand 02. The cross plot of the effective porosity (ϕ_e) versus volume of shale (Vsh) that was carried out, reveals a decrease in the effective porosity with an increase in shale volume. This depicts a laminated shale pattern across the entire reservoir sands. The petrophysical estimation of water saturation from the conventional method and the Shaly-sand models of Simandoux and Indonesia, show a clear disparity in water saturation. This disparity recorded, was attributed to the degree of shaliness that is associated with the reservoirs, suggestive of over estimation of water saturation of the reservoirs by the conventional model.

Keywords: Conventional, Indonesia, Simandoux, Water saturation.

1. Introduction

The pore spaces in the subsurface that form the reservoir rocks are always completely saturated with fluids. These fluids are associated with sediments deposition, i.e. water filling the pores spaces during deposition and buoyance effect from oil and gas migration to the reservoir rock. This is made possible through porous and permeable rocks from nearby organic rich shale, resulting in partial displacement of saturated water from the pore spaces of the reservoir rocks.

Water saturation is an important petrophysical parameter that is used in the quantification of the hydrocarbon content of reservoir rocks. Water saturation (S_w), is the fraction of the pore volume occupied by water [1]. Improper calculation of water saturation leads to great errors in hydrocarbon saturation ($1-S_w$) estimation. There are several methods to determine water saturation some of which include dielectric measurements, nuclear measurements, the ratio technique (SP vs R_{xo}/R_t), crossplots, F-overlays, Archie's equation and shaly sand methods.

The presence of clays (shale) in formations results in the reduction of their 'True Resistivity' (R_t) values [2]. This makes the value of water saturation to appear higher than what it should be, in turn suggesting a lower hydrocarbon saturation volume (Recall $S_h = 1 - S_w$).

In 'clean formations,' i.e. sands devoid of clay or with less than 15% clay, water saturation is best obtained using the conventional Archie equation which is expressed in terms of 'True Resistivity' [3]. However, the Archie equation fails in shaly sands because the wet rock conductivity (C_o) is not linearly related to the water conductivity (C_w). This is due to the excess conductivity caused by the clay content of the formation and fresh formation water as showing in Figure-1, leading to the overestimation of water saturation since the excess clay conductivity is not taken into consideration [1].

*Email: emexabbey@gmail.com

Unlike 'clean formations' where the formation water serves as the only electrically conductive medium, the shaly sand model has to deal with both the conductivity of the clay minerals in the rock matrix and also that of the formation water. As more and more studies and experiments are carried out in a bid to understand clay-mineral-rich rocks, more complicated electrical models are developed to account for the effects of the geometries of conductive clay minerals and shale on rock resistivity. The primary goal of the shaly-sand models is to determine a working relationship between S_w models using parameters similar to the Archie model, but also incorporating the quantity and specific electrical properties of the clay-mineral/shale. All of the shaly-sand models reduce to the Archie equation when the shale component is zero [4].

To properly evaluate shaly-sand reservoir, there is a need to take into account the shale/clay distribution in the formation, this guides the interpretation on the type of model to employ. Shaly sand reservoirs can have any of three different clay distributions viz: (i) **Laminated** when the shales are found as intercalations between sand units, (ii) **Structural** when they exist as grains or nodules in the formation matrix and (iii) **Dispersed** when the shales are dispersed throughout the sand unit, partially filling the intergranular interstice [5].

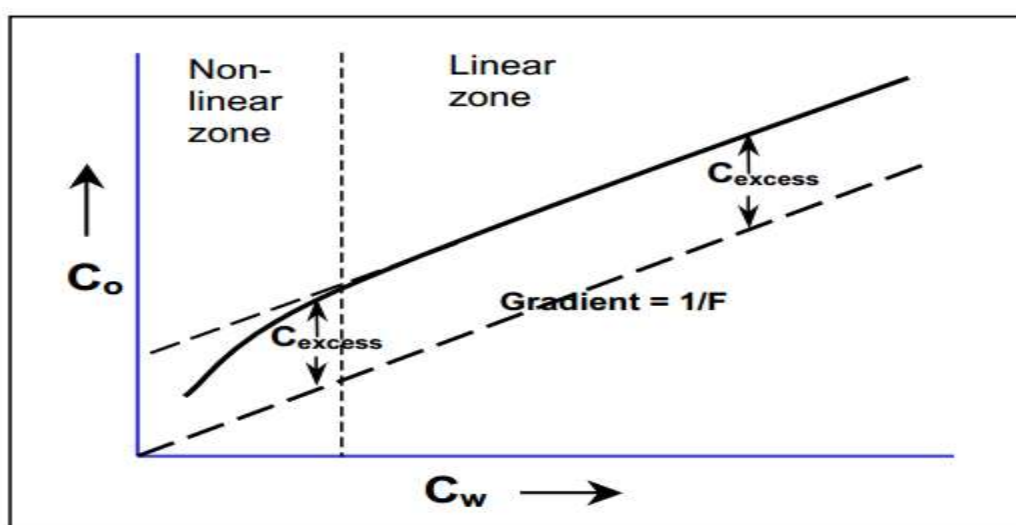


Figure 1-Variation of wet rock conductivity, C_o and water conductivity, C_w as a Result of Shaliness Effect (from Bateman, [1])

The Study Area

The Niger Delta is the dominant sedimentary basins in Nigeria by its size and economic importance. The delta covers an area of about 105,000 km² [6]. The Niger Delta is situated in the Gulf of Guinea on the West Coast of Africa. It is located at the southeastern end of Nigeria, bordering the Atlantic Ocean and extends from around latitudes 4° to 6°N and longitudes 3° to 9°E. The association of source rock, lithology types, structures and thermal histories were some of the conditions favorable for the generation, accumulation and retention of hydrocarbon in the Niger Delta, thus making the Delta very prolific in terms of hydrocarbon occurrence [7].

The studied field, TN field is located offshore Niger Delta with an area of 52 km². The Niger Delta is a wave-dominated delta and is composed of an overall regressive clastic sequence which reaches a maximum thickness of about 12 km in the basin center. The Delta's sediments show an upward transition from marine pro-delta shales (Akata Formation) through a paralic interval (Agbada Formation) to a continental sequence (Benin Formation). These three sedimentary environments, typical of most deltaic environments extend across the whole delta and ranges in age from Early Tertiary to Recent. The offshore Niger Delta has the characteristic shelf slope break of growth fault modified ramp margins [8].

Trap configuration in the offshore Niger Delta is controlled by gravity driven systems of linked extensional growth faults and compressional toe thrusts initiated during the Paleocene when the modern Niger Delta was formed. Oil and gas are predominantly trapped structurally (roll over anticlines and fault closures) and stratigraphically (paleochannel fills, regional sand

pinch-outs and truncations, crestal accumulations below unconformity surfaces, canyon-fill accumulations above unconformity surfaces) [9,10]. Figure-(2a, 2b) shows the geographical location of Niger Delta in Gulf of Guinea and Niger Delta Province outline with the well locations in the study field respectively.

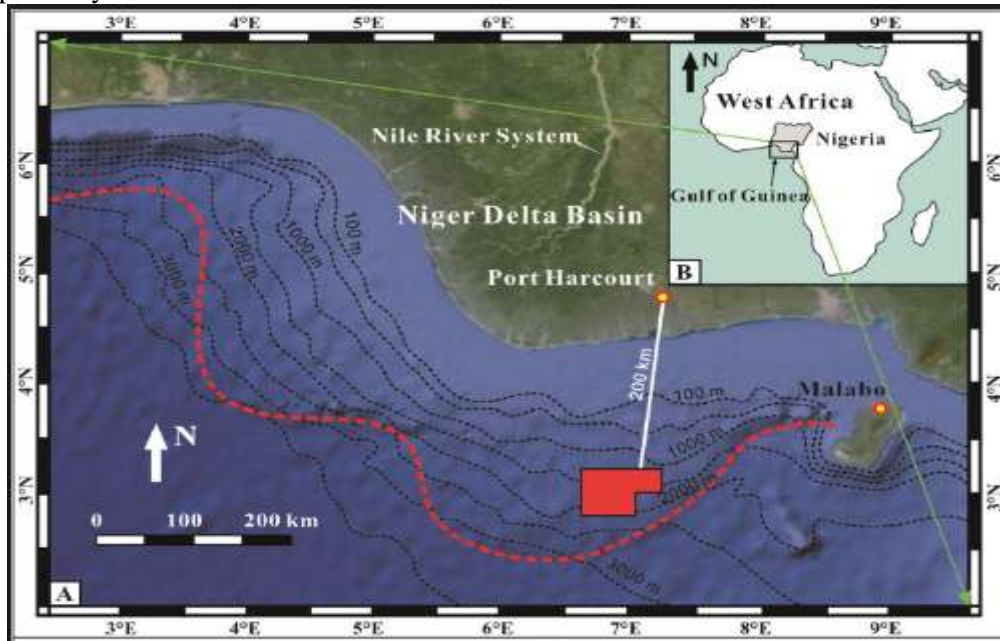


Figure 2a-Geographical Location of Niger Delta in Gulf of Guinea.

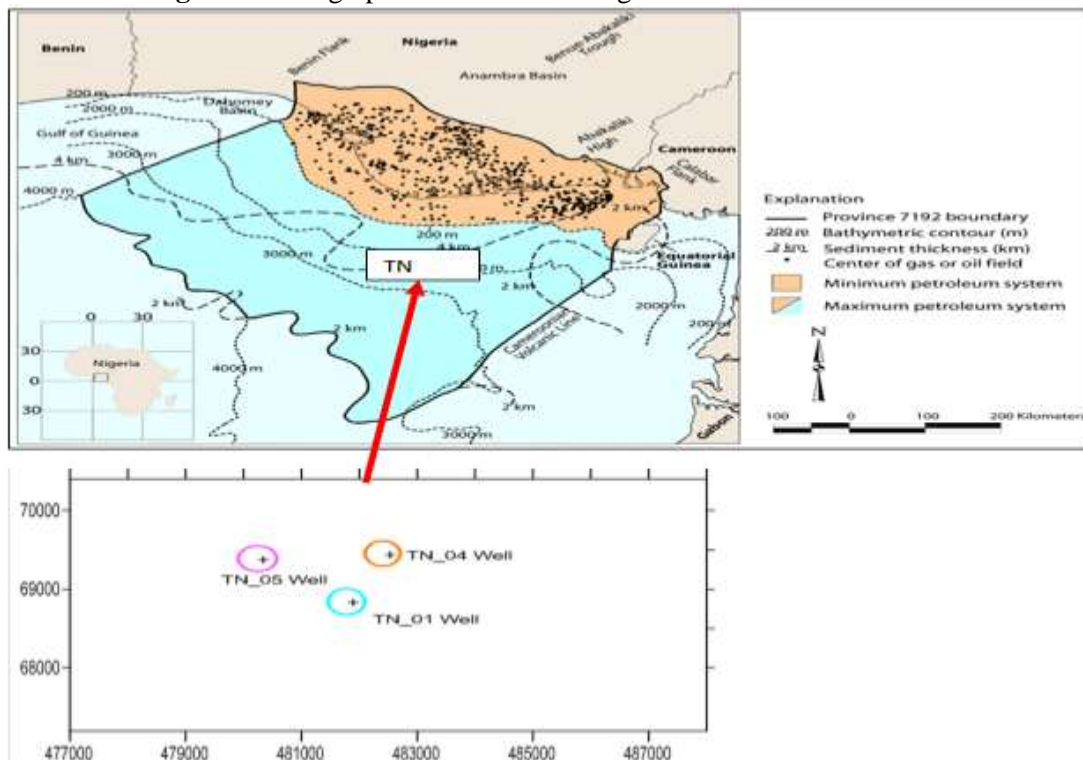


Figure 2b-The Niger Delta Province Outline (after Tuttle *et al.*, [11]) and Well Locations in the Studied TN Field.

2. Materials and Method

The data used in this research were obtained from TN field, offshore Niger Delta. The data contains Gamma Ray, Resistivity, Neutron-Density logs from three (3) Wells TN_01, TN_04 and TN_05. Each well was first evaluated and potential reservoir (sand) units were marked out using the log motif/signature from the gamma ray log of three wells. The wells were then correlated and reservoir

units were mapped across the wells with the help of thick marker shales that were observed in the wells. The mapped sands were named Sand_01 and Sand_02 with the latter (Sand_02) appearing to have pinched out between wells TN_04 and TN_05. The two reservoirs sand are stratigraphical separated by the thick shale marker, making it practical impossible for the fluid content of the two reservoirs to interact with each other since the marker shale serves as a seal to both reservoirs.

The volume of shale (V_{sh}) was calculated using both linear [12] equation 2.1 and nonlinear equations, Steiber [13] equation 2.2.

$$V_{shgr} = \frac{Gr_{log} - Gr_{clean}}{Gr_{clay} - Gr_{clean}} \quad \text{Linear (Asquith and Krygowski, [12])} \quad 2.1$$

$$V_{shst} = \frac{V_{shgr}}{3.0 - 2.0 V_{shgr}} \quad \text{Nonlinear (Steiber)} \quad 2.2$$

The nonlinear V_{sh} was used since it predicted a lower volume of shale. The density porosity was calculated from equation 2.3 Davis [14], while the 'Total porosity' value was calculated using the root mean square method (RMS) in equation 2.4 Davis [14] as is usually the case when the interval of interest is a hydrocarbon bearing formation.

$$\phi_d = \frac{2.65 - \rho_b}{2.65 - \rho_f} \quad 2.3$$

$$\phi_{nd} = \sqrt{\frac{\phi_n^2 + \phi_d^2}{2}} \quad 2.4$$

Effective porosity was then calculated from the total porosity using equation 2.5 Davis [14].

$$\phi_e = \phi_T - V_{sh} * \phi_T \quad 2.5$$

Where; V_{shgr} = volume of shale gamma (linear), V_{shst} = volume of shale ((Steiber) nonlinear), Gr_{log} = gamma ray log reading in zone of interest corrected for borehole size, Gr_{clean} = gamma ray log reading in 100% clean zone, Gr_{clay} = gamma ray log reading in 100% shale, ϕ_d = density porosity, ρ_b = density log reading in zone of interest, ρ_f = density log reading in 100% water, ϕ_n = Neutron porosity, ϕ_T = total porosity, ϕ_{nd} = neutron-density porosity.

The shale model was determined from the plot of effective porosity against volume of shale and was compared after Chevron guide [15] Figure-3. The plots show that both reservoir sands contain laminated shale. This necessitated the use of the Simandoux and Poupon-Leveaux (Indonesia) models for S_w determination. The conventional Archie method was also used to calculate the water saturation in order to confirm the earlier assertion that it over estimates water saturation in shaly sand reservoirs.

$$S_w = \frac{aR_w}{2\phi_e^m} \left\{ -\frac{V_{sh}}{R_{sh}} + \left[\left(\frac{V_{sh}}{R_{sh}} \right)^2 + \frac{4\phi_e^m}{aR_w R_T} \right]^{0.5} \right\} \quad \text{Simandoux} \quad 2.6$$

$$S_w = \left\{ \left[\left(\frac{V_{sh}^2 - V_{sh}}{R_{sh}} \right)^{\frac{1}{2}} + \left(\frac{\phi_e^m}{R_w} \right)^{\frac{1}{2}} \right]^2 R_T \right\}^{\frac{1}{n}} \quad \text{Poupon-Leveaux (Indonesia)} \quad 2.7$$

Where a = tortuosity exponent, V_{sh} = shale volume, R_T = deep resistivity log reading, R_{sh} = resistivity of the adjacent shale, ϕ_e = effective porosity, m = cementation exponent, R_w = water resistivity at formation temperature

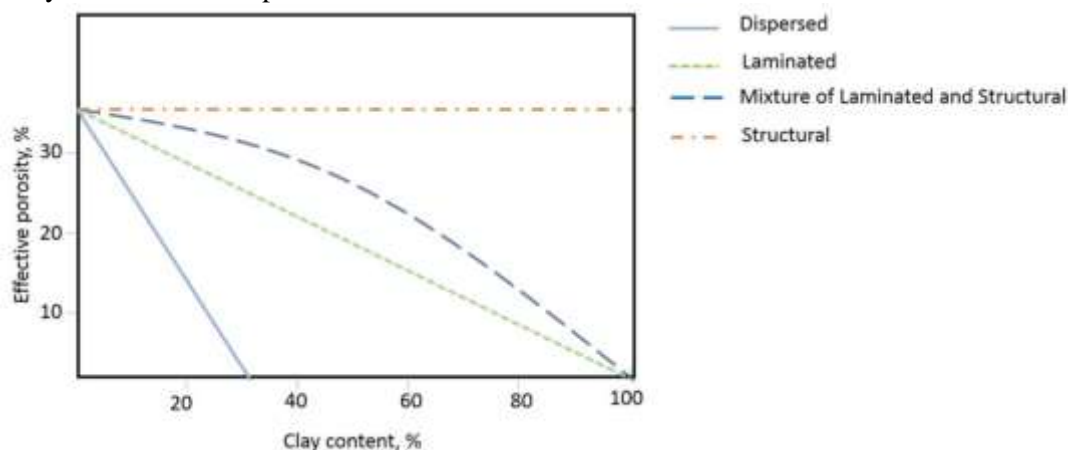


Figure 3-Graph of Effective Porosity Against Clay Content (after Chevron Guide, [15]).

3. Results and Discussion

Figure-4 shows the correlation of the wells. Figure-5 is a cross plot of effective porosity against V_{sh} while Figure-6 is graphical representation of water saturation model from the Wells. The results of all the three (3) well sections are shown in Figures-(7-11). Table-1 displays the estimated effective porosity and water saturation from the Wells. Figure-12 illustrates a regression line showing the coefficient of correlation between Simandoux and Indonesia model for the two mapped reservoir Sand 01 and Sand 02.

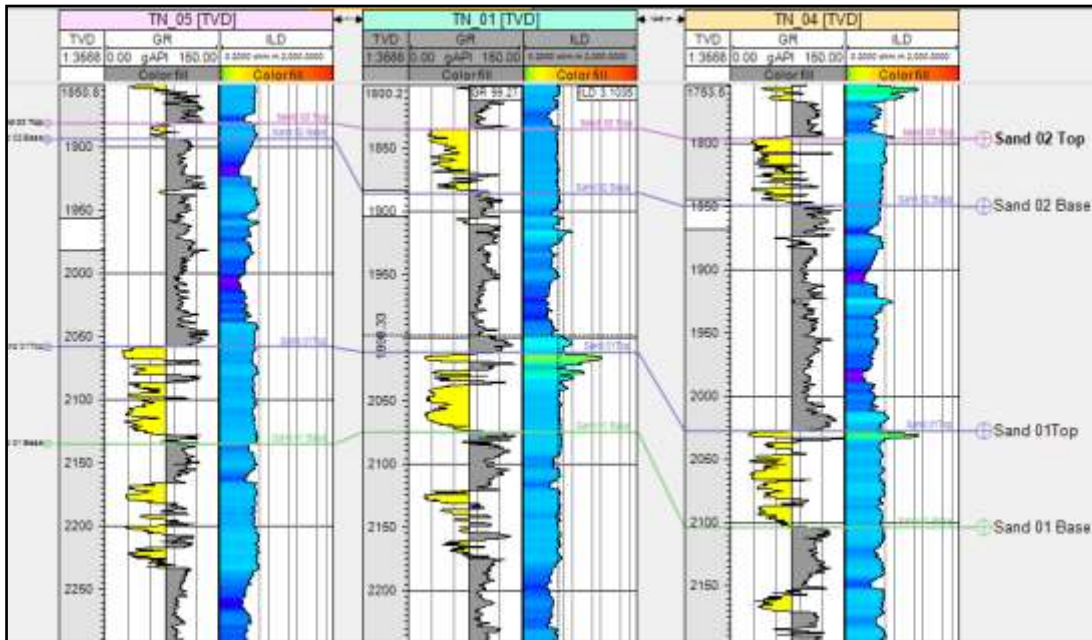


Figure 4-Stratigraphic Correlation of TN-05, TN_01 and TN_04 Wells in the Field.

Clay Distribution

The result obtained from the cross plot of Effective porosity against volume of shale Figure-5, depicts a model of laminated shale with a decrease in effective porosity and increase in volume of shale, when compared with Figure-3. This lamination is as a result of fine grained particles settling within deposited sediments forming fine lamina across the beds. These are often seen as discrete thin beds sandwiched in between sandstones. The pore spaces and its connectivity in these reservoir are reduced due to the presence of shale lamina. This in turns reduces the porosity of the reservoir sand and it brings about decrease in its resistivity due to the presence of clay properties.

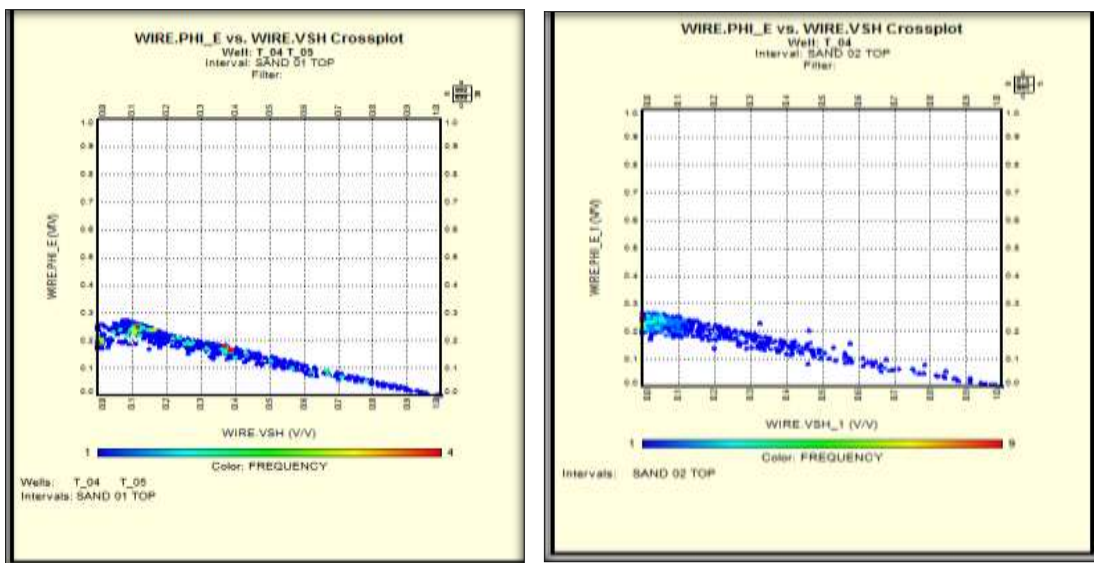


Figure 5-Cross Plot of Effective Porosity Against Volume of Shale (V_{sh}) Depicting Laminated Shale Model.

Reservoir Sand 01

In Well TN_1, Sand_01 has a net pay thickness of 112.4 ft with total porosity of 0.24 and effective porosity of 0.21. From conventional Archie water saturation method, 0.24 was obtained for S_w while the shaly sand models of Simandoux and Indonesia gave 0.08 and 0.11 respectively. This shows that the conventional model estimates water saturation by over 100% compared to the shaly sand models used.

In Well TN_4, Sand_01 has a reservoir thickness of 119.3 ft having a total porosity of 0.23 and effective porosity of 0.16. The conventional model estimates water saturation to be 0.22 compared with the Simandoux and Indonesia models which returned 0.09 and 0.13 respectively for water saturation. This is also in line with what was observed from the same sand in Well TN_1.

In Well TN_5, Sand_01 has a porosity of 0.24 and effective porosity of 0.17 but unlike the earlier instances in Wells TN_01 and TN_04, the water saturation values from the conventional and shaly sand models are quite close with Archie having 0.11 while the shaly sand models of Simandoux and Indonesia returned 0.08 and 0.09 respectively. From the well section shown in Figure-9 it can be seen that they actually tracked at some point.

Reservoir Sand 02

In well TN_1, Sand_02 reservoir has a thickness of 187.5 ft with porosity and effective porosity being 0.24 and 0.21 respectively. From the conventional method, the water saturation is estimated as 0.69 while Simandoux and Indonesia recorded 0.32 and 0.34 respectively for S_w . The high difference in conventional and shaly sand model is vivid in the displayed well section of Figure-10.

Sand_02 reservoir of TN_2 well shows a water saturation of 0.55 and 0.59 from the Simandoux and Indonesia models respectively compared to the conventional method with 0.89. The porosity associated with this reservoir is 0.25 with an effective porosity of 0.20. The reservoir exhibits a low resistivity contrast which is associated with the overestimation of water resistivity (R_w) by the conventional Archie model. By careful examination of the reservoir from the well track it can be seen that there is a negative separation of the density and neutron traces which is indicative of hydrocarbons.

The regression correlation coefficient between the Simandoux and Indonesia in reservoir Sand 01 and Reservoir Sand 02 indicates that the two are suitable for this field with their water saturation prediction. For sand 01 and 02 we have 0.945 and 0.976 respectively indicative of good correlation with both. Although this test was not drawn for the conventional Archie with the shaly sand model of Simandoux and Indonesia because the case of over estimation is wildly pronounced in all the two reservoir sands in the three wells used.

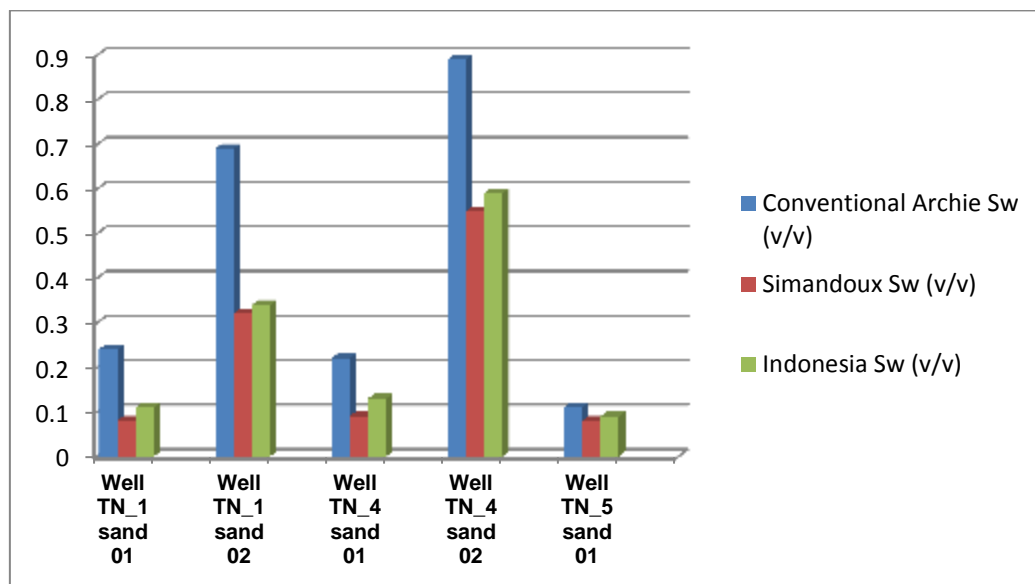


Figure 6-Graphical Representation of Water Saturation Model from the Wells.

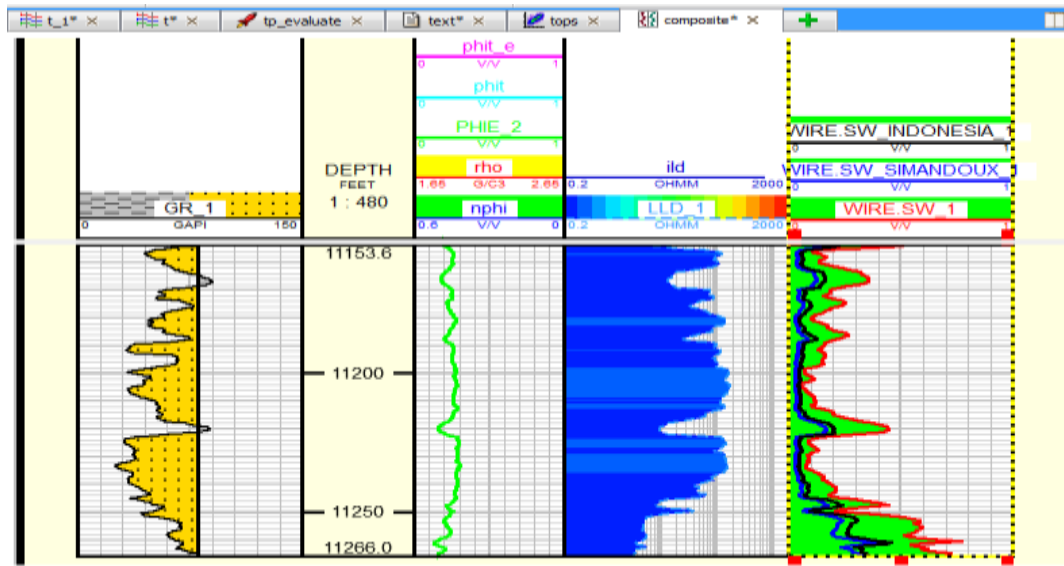


Figure 7-Well TN_01 Sand 01 Showing the Estimated Water Saturation Logs.

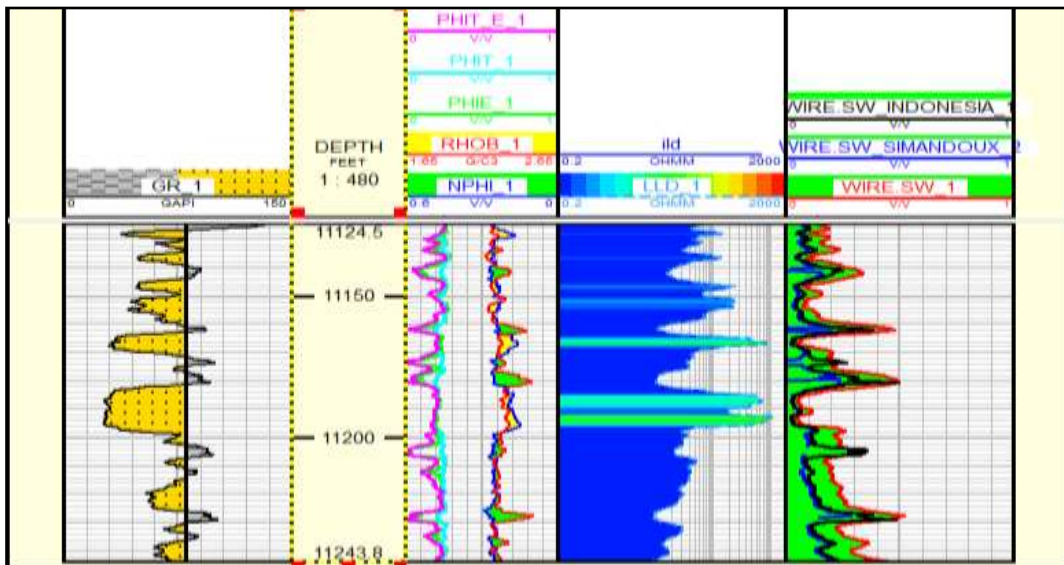


Figure 8-Well Tn_04 Sand 01 Showing Estimated Water Saturation Logs

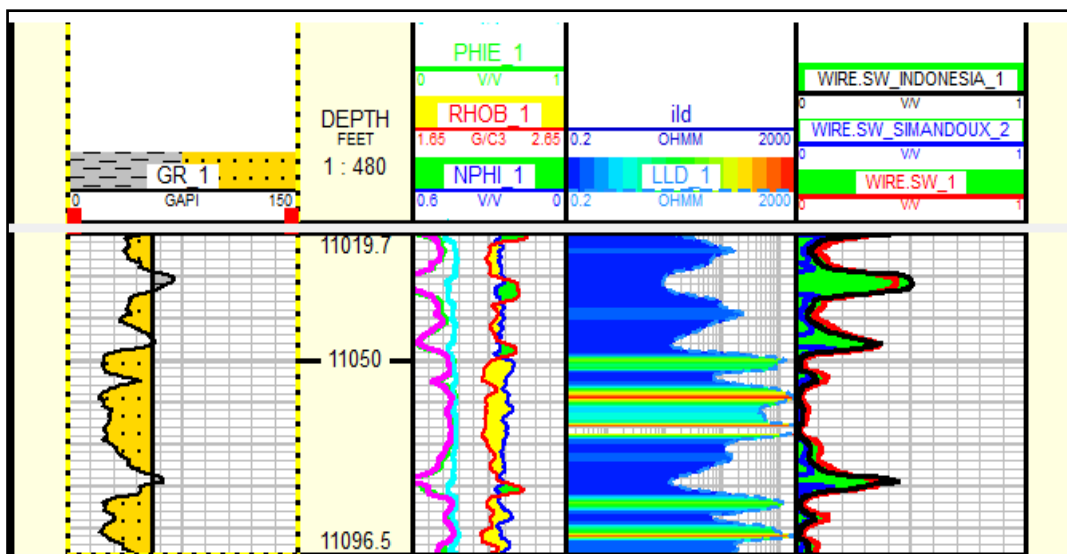


Figure 9-Well TN_05 Sand 01 Showing the Estimated Water Saturation Logs

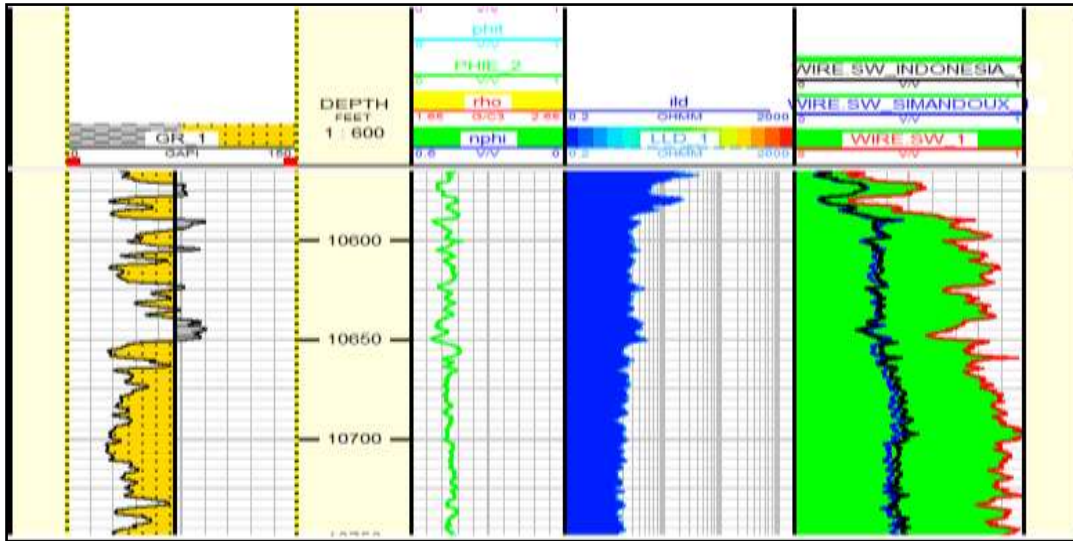


Figure 10-Well TN_01 Sand 02 Showing the Estimated Water Saturation Logs

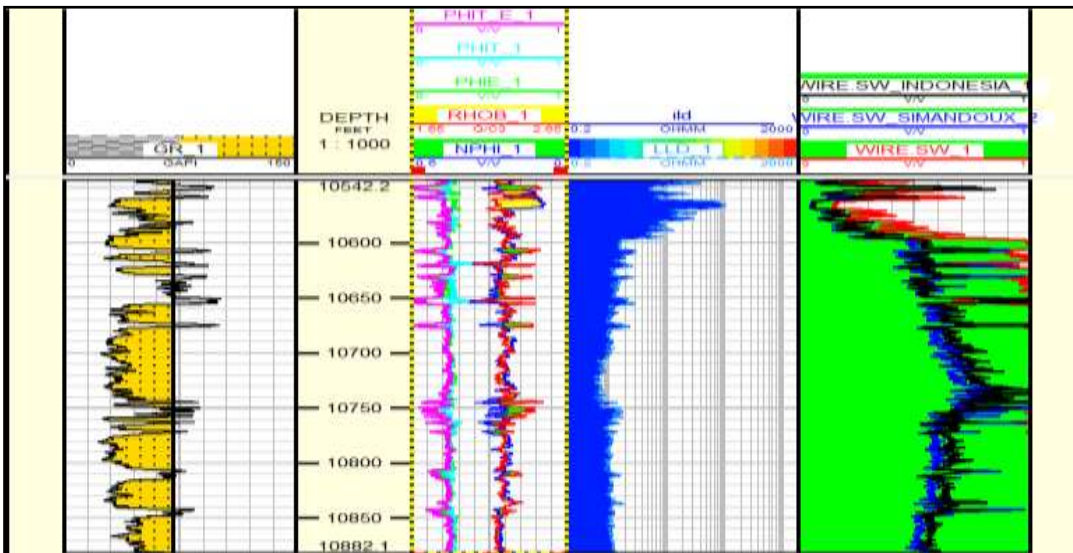


Figure 11-Well TN_04 Sand 02 Showing the Estimated Water Saturation Log

Table 1-The Estimated Effective Porosity and Water Saturation Values from the Wells

Mapped Reservoir Sands	Reservoir Thickness (ft)	Porosity (v/v)	Effective porosity(v/v)	Conventional Archie Sw (v/v)	Simandoux Sw(v/v)	Indonesia Sw(v/v)
Well TN_1 sand 01	112.4	0.24	0.21	0.24	0.08	0.11
Well TN_1 sand 02	187.5	0.24	0.21	0.69	0.32	0.34
Well TN_4 sand 01	119.3	0.23	0.16	0.22	0.09	0.13
Well TN_4 sand 02	339.9	0.25	0.20	0.89	0.55	0.59
Well TN_5 sand 01	76.8	0.24	0.17	0.11	0.08	0.09

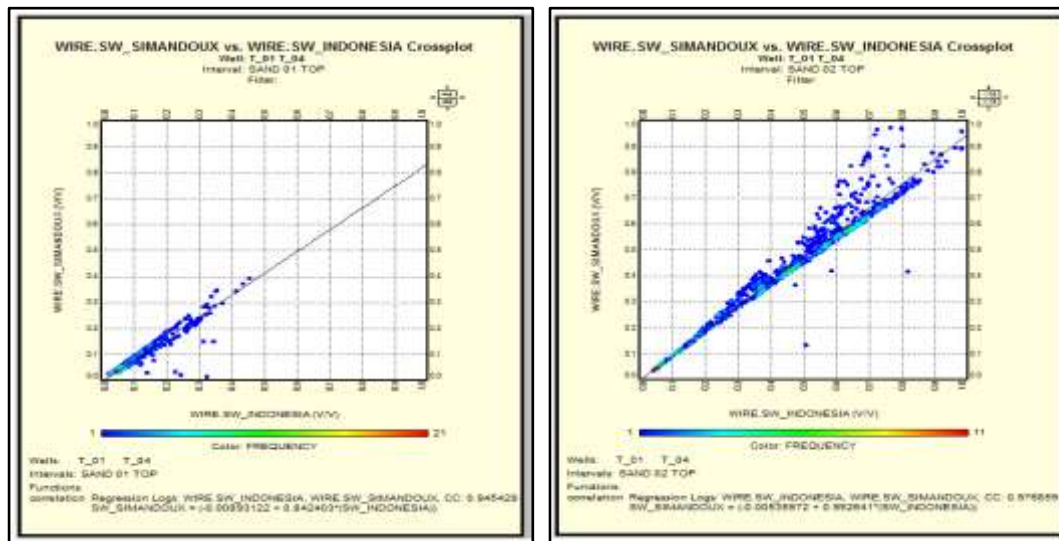


Figure 12-A Regression Line Drawn to Show the Coefficient of Correlation between Simandoux and Indonesia Model for the Two Mapped Reservoirs, Sand 01 and Sand 02 respectively in the wells.

4.0 Conclusion

Two reservoir sands were delineated in this study namely Sand 01 and Sand 02. Sand 01 was mapped across the three wells (TN_01, TN_04 and TN_05) while Sand 02 cut across TN_01 and TN_04 wells. Reservoir sand 01 had a thickness of 112.4 ft in TN_1, 119.3 ft in TN_04 and 76ft in TN_05 while Sand 02 had a thickness of 187.5 ft and 339.9 ft for TN_01 and TN_04 respectively.

The clay distributions as observed from the reservoirs in Figure-5 depict laminated models with a decrease in in effective porosity with an increase in the volume of shale. This lamination is as a result of fine grained particles settling within deposited sediments forming fine lamina across the beds. These are often seen as discrete thin beds sandwiched in between sandstones. The pore spaces and its connectivity in these reservoir are reduced due to the presence of shale lamina. This in turns reduces the porosity of the reservoir sand and brings about decrease in its resistivity due to the presence of clay properties which are conductive in nature. With the presence of this shaliness, the conventional method appears to overestimate water saturation since it failed to recognize the lamina in the reservoirs and also its calculation is based on total porosity and not effective porosity. The total porosity of the two sand bodies across the three wells range from 23% to 25%, while the effective porosity of the reservoir sands stood at 16% to 21% due to the clay laminations encountered in the zones.

The result obtained revealed overestimated Sw by over 100% for Sand 01 and by 50% in Sand 02 by conventional model while as against the Shaly Sand models of Simandoux and Indonesia in this field due to the presence of shaliness in the studied reservoirs

5. References

1. Bateman, R. M. **1985**. *Open hole Log Analysis and Formation Evaluation*. IHRDC, Publishers, 137 Newbury Street, Boston USA.
2. Djebbar, T. and Erle, C. D. **2012**. *Theory and Practice of Measuring Reservoir Rock and Fluid transport Properties*. Gulf professional publishing, 225 Wyman Street, Waltham MA 02451 USA.
3. Archie, G. E. **1942**. The Electrical Resistivity Log as an Aid in Determining Some Reservoir Characteristics" *Petroleum Transactions of the AIME*146
4. Petrowiki **2015**: http://petrowiki.org/Water_saturation_determination
5. Schlumberger **1989**. *Log Interpretation Principles / Applications*. Schlumberger Well Services, Houston. 241
6. Avbovbo, A. A. **1978**. Tertiary Lithostratigraphy of Niger Delta. *American Association of Petroleum Geologists*, Tulsa, Oklahoma: **10**(14): 96-200.

7. Odebeatu, A. and Alexander, G. **2006**. Application of Spectral Decomposition to Detection of Dispersion Anomalies Associated with Gas Saturation. *The Leading Edge*, **25**: 205-210
8. Aizebeokhai, A. P, and Olayinka, I. **2011**. Structural and stratigraphic mapping of Emi field, offshore Niger Delta. *Journal of Geology and Mining Research*, **3**(2): 25-38,
9. Orife J. M, and Avbovbo, A. **1982**. Stratigraphic and unconformity traps in the Niger Delta, in T. Halbouty, ed., the deliberate search for subtle trap: *Am. Assoc. Petrol. Geol. Memoir*, **32**: 251-265.
10. Kruiise, H. R, and Idiagbor, A. **1994**. Stratigraphic traps in the Eastern NigerDelta: Innovatory and concepts. *Nig. Assoc. Petrol. Explo. Bull.*, **9**:76-85.
11. Tuttle, M. L. W., Charpentier R. R. and Brownfield, M. E. **1999**. The Niger Delta Petroleum System: Niger Delta Province, Nigeria, Cameroun and Equatorial Guinea, Africa: USGS Open-File Report 99 - 50H.
12. Asquith, G. and Krygowski, D. **2004**. Basic Well Log Analysis: AAPG Methods in Exploration **16**: 31-35.
13. Stieber, S. J. **1970**. Pulsed Neutron Capture Log Evaluation - Louisiana Gulf Coast. *Society of Petroleum Engineers*. doi:10.2118/2961-MS
14. Davis, D.H. **1954**. Estimating Porosity of Sedimentary Rocks from Bulk Density. *The Journal of Geology*, **62**(1): 102-107
15. Chevron Guide. **1996**. Sandstone Reservoir Evaluation: Sandstone Characteristics, presented at the Intermediate Formation Evaluation Seminar held in Ibadan, Nigeria. August 25 – 31, 1 – 44.